科学通报 2025 年 第 70 卷 第 6 期: 729 ~ 736
高性能铅锡硫族热电材料专辑 论 文
《中国科学》杂志社 SCIENCE CHINA PRESS

掺杂Cd元素协同优化$Sb_2Te_3(SnTe)_6$的热电输运性能

刘雨晴, 崔金华, 王淑芳*, 钱鑫*

河北大学物理科学与技术学院, 河北省光电信息材料重点实验室, 保定 071002

* 联系人, E-mail: sfwang@hbu.edu.cn; qianxin@hbu.edu.cn.

2024-07-17 收稿, 2024-08-13 修回, 2024-08-16 接受, 2024-08-19 网络版发表

国家自然科学基金(52102234)、河北省教育厅科学研究项目(QN2024263)、河北大学高层次人才科研启动项目(521000981421)和河北省光电信息材料实验室绩效补贴基金(22567634H)资助

摘要 环境友好型的热电材料碲化锡(SnTe)因不含有毒元素铅(Pb)而受到广泛关注和研究. 由于其具有极高的载流子浓度, 尽管在中高温区表现出较高的热电性能, 但其近室温区的热电性能很难提升. 随着热电制冷技术的发展, 材料在近室温区的热电性能显得更加重要. 之前的研究表明, 合金化Sb_2Te_3可以引入大量的阳离子空位和位错缺陷, 能有效抑制SnTe的晶格热导率, 同时还可以调控其能带结构增大有效质量, 是提高其宽温域热电性能的有效策略. 本研究在合金化Sb_2Te_3的基础上, 通过在Sn位掺杂Cd元素, 协同调控了$Sb_2Te_3(SnTe)_6$的载流子浓度、态密度有效质量和晶格热导率. 最终$Sb_2Te_3(Sn_{0.96}Cd_{0.04}Te)_6$在300 K的$ZT$值达到了0.26, 323~773 K温度范围内的平均ZT值达到了0.79, 表明SnTe-Sb_2Te_3化合物在热电发电和制冷领域具有重要的应用潜力.

关键词 热电材料, 载流子浓度, 有效质量, 晶格热导率, 热电性能

在能源危机持续加剧的背景下, 全球范围内对高效且环保的能源转换方法的需求日益迫切. 热电材料作为一种能够实现热能与电能双向转换的功能性材料, 在废热利用、固态制冷技术等领域展现出巨大的应用潜力, 为当前能源短缺问题提供了创新性的解决方法[1~3]. 热电器件的转换效率主要取决于材料的无量纲热电优值(ZT), 其计算公式为$ZT=S^2\sigma T/\kappa_{tot}$, 式中$S$代表塞贝克系数, σ表示电导率, T是绝对温度, κ_{tot}为材料的总热导率[4~6]. 高效热电转换材料需同时具备优异的电输运性能(功率因子, PF=$S^2\sigma$)和较低的总热导率. 然而, 这些热电参数之间存在显著的相互依赖与协同作用, 很难通过单独优化某个参数实现热电性能的提升[7~9].

SnTe与PbTe有着相同的晶体结构和相似的双价带结构, 且不含有毒元素Pb, 被认为是一种极具应用潜力的绿色环保型热电材料[10~13]. 但是, SnTe较小的带隙导致其在高温容易发生双极扩散现象, 同时极高的空穴载流子浓度(10^{20}~10^{21} cm^{-3})和较大的轻重价带能量差(0.35 eV)导致SnTe的塞贝克系数较低. 此外, 较高的晶格热导率导致SnTe在近室温附近的热电性能很难提升. 针对这些问题, 科研人员探索了多种方法以提高SnTe的热电性能[14~16]. 例如, 进行施主元素掺杂降低载流子浓度[17~19], 通过元素固溶促进价带收敛提高态密度有效质量[20,21], 利用熵工程引入全尺度缺陷结构降低晶格热导率[22]等.

近年来, 空位工程[23]作为一种新兴的优化策略, 凭借其独特的声子散射机制和能带调控能力, 逐渐得到了科研工作者的广泛关注. 具体而言, 该方法通过在SnTe中合金化Sb_2Te_3人为地引入阳离子空位, 进而构建位错等缺陷结构, 这些结构可以有效地散射多频段的声子, 显著降低材料的晶格热导率. 同时, 合金化Sb_2Te_3还能够调整能带结构, 显著提升SnTe的功率因子[24~26]. 2020年, Xu等人[27]发现在SnTe中合金化Sb_2Te_3可以构

引用格式: 刘雨晴, 崔金华, 王淑芳, 等. 掺杂Cd元素协同优化$Sb_2Te_3(SnTe)_6$的热电输运性能. 科学通报, 2025, 70: 729–736
Liu Y Q, Cui J H, Wang S-F, et al. Synergistic optimization of thermoelectric transport properties in $Sb_2Te_3(SnTe)_6$ through Cd doping (in Chinese). Chin Sci Bull, 2025, 70: 729–736, doi: 10.1360/TB-2024-0776

© 2024《中国科学》杂志社

建范德华面间隙结构, 显著降低晶格热导率. 随后, 他们在合金化的基础上掺杂Re元素进一步调节载流子浓度, 最终$Sb_2Te_3(Sn_{0.996}Re_{0.004}Te)_{10}$在773 K的最高$ZT$值达到了1.4. 2023年, 该课题组[28]通过补偿阳离子空位的方法进一步提高$Sb_2Te_3(SnTe)_{10}$的载流子迁移率, 最终$Sb_2Te_3(SnMn_{0.08}Te)_{10}$在773 K的最高$ZT$值达到了1.3, 300~823 K温度范围内的平均ZT值达到了0.78.

随着热电制冷技术在各个领域的应用日益广泛, 材料在近室温范围的热电性能显得尤为重要[29]. 鉴于$Sb_2Te_3(SnTe)_6$在近室温区表现出更优异的热电性能[23], 因此选择在该材料基础上进行优化, 以进一步提升其宽温域的热电性能. 本研究通过在Sn位掺杂Cd元素, 协同优化了$Sb_2Te_3(SnTe)_6$的载流子浓度和态密度有效质量, 材料的热电输运性能在整个温度范围得到显著提升, 室温功率因子由$Sb_2Te_3(SnTe)_6$的8.54 μW cm^{-1} K^{-2}提升至$Sb_2Te_3(Sn_{0.96}Cd_{0.04}Te)_6$的10.95 μW cm^{-1} K^{-2}, 在300~773 K温度范围的平均功率因子高达17.42 μW cm^{-1} K^{-2}. 最终$Sb_2Te_3(Sn_{0.96}Cd_{0.04}Te)_6$样品在300 K的$ZT$值达到了0.26, 323~773 K的平均$ZT$值达到了0.79, 显著提高了SnTe基材料在宽温域范围的热电性能.

1 实验

1.1 材料制备

采用高温熔融法和放电等离子烧结技术(spark plasma sintering, SPS)制备了$Sb_2Te_3(Sn_{1-x}Cd_xTe)_6$ (x=0~0.08)样品. 首先, 将具有高纯度(>99.99%)的Sn、Sb、Te、Cd颗粒按照以上化学计量比进行称量, 放入石英管后进行抽真空, 当真空度达到~10^{-4} Pa时将石英管进行火焰密封. 将密封后的石英管放入马弗炉中进行高温熔融反应, 由室温在16 h内缓慢加热至1423 K并保温24 h, 然后在8 h降温至873 K继续保温6 h, 然后随炉冷却至室温. 将反应完成的铸锭在研钵中研磨成颗粒均匀的粉末, 放入直径为15 mm的石墨模具中, 在烧结温度为823 K、烧结压力为50 MPa的条件下进行放电等离子烧结, 烧结时间为5 min, 最终获得高密度的圆柱形块体样品进行后续性能测试.

1.2 结构表征

将烧结后的块体样品研磨成均匀的粉末, 使用Cu Kα辐射的X射线衍射仪(Bruker D8 Advance)对粉末样品进行物相结构表征, 测试范围为20°~80°, 步长值为0.02°, 停留时间为0.1 s. 使用扫描电子显微镜(Nova Nano SEM 450)观察块体样品的微观形貌, 通过X射线能谱仪(energy dispersive spectrometer, EDS)分析材料的元素分布.

1.3 热电性能测试

将烧结后的圆柱形样品使用线切割机切割成3×3×15 mm^{3}的长方体, 使用LINSEIS公司的电输运性能测试系统(LSR3-1000, Germany)测试样品的电阻率和塞贝克系数, 测试温度范围为300~773 K. 为了防止测试时高温下样品挥发对仪器设备造成损害, 在进行测试前需要将样品除测试面外的其他表面均匀喷涂一层薄薄的氮化硼(BN). 将烧结后的样品切割成8 mm×8 mm、厚度约为1 mm的正方形, 使用霍尔系数测试系统(Hall-TH6402)测试室温下样品的霍尔载流子浓度和载流子迁移率. 将烧结后的样品切割成边长8×8 mm^2、厚度约为1.5 mm的正方形, 使用LINSEIS公司的激光热导仪(LFA 1000)测试样品的热扩散系数(D), 测试方法为激光闪射法. 根据公式$\kappa_{tot}=C_p\times D\times\rho$计算材料的总热导率, 式中$\rho$为通过质量和体积计算的样品密度, C_p是根据Dulong-petit定律计算的样品比热容: $C_p=3NR/M$, 其中N为原子数, R为气体常数, M为相对分子质量. 考虑温度的影响, 温度每升高100 K, 样品的C_p增加1%.

2 结果与讨论

2.1 晶体结构表征

图1展示了$Sb_2Te_3(Sn_{1-x}Cd_xTe)_6$ (x=0~0.08)样品的X射线衍射(X-ray diffraction, XRD)图谱和晶格常数随Cd掺杂含量的变化, 所有样品的布拉格衍射峰均与立方岩盐结构一一对应, 没有明显的第二相杂峰出现. 随着Cd掺杂含量的增加, 晶格常数逐渐减小, 这主要是由于Cd^{2+}的离子半径小于Sn^{2+}的离子半径, 符合Vegard定律, 表明Cd元素已成功进入到样品的晶格中. 图2是$Sb_2Te_3(Sn_{0.96}Cd_{0.04}Te)_6$样品的抛光表面扫描电子显微镜(scanning electron microscopy, SEM)图以及对应的EDS图谱, 结果表明Sn、Sb、Te、Cd元素在样品中均匀分布, 没有观察到明显的元素偏析和第二相纳米结构, 与XRD的测试结果保持一致.

2.2 电输运性能

图3是$Sb_2Te_3(Sn_{1-x}Cd_xTe)_6$ (x=0~0.08)样品的电输

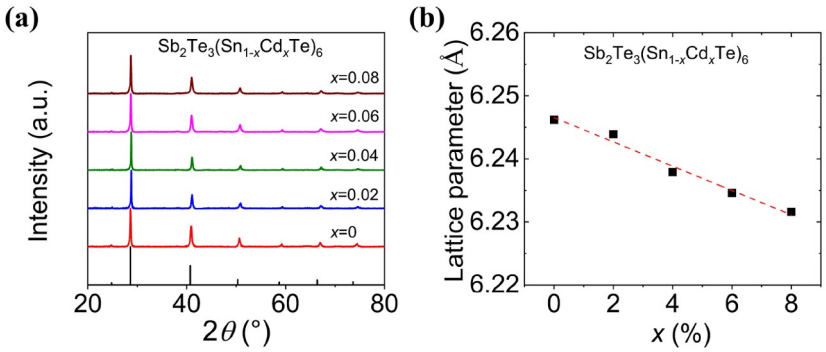


图 1 (网络版彩色)样品$Sb_2Te_3(Sn_{1-x}Cd_xTe)_6$ (x=0~0.08)的粉末XRD图谱(a), 以及晶格常数随Cd元素掺杂含量的变化(b)
Figure 1 (Color online) Powder XRD patterns for $Sb_2Te_3(Sn_{1-x}Cd_xTe)_6$ (x=0–0.08) (a), and calculated lattice parameters as a function of Cd content (b)

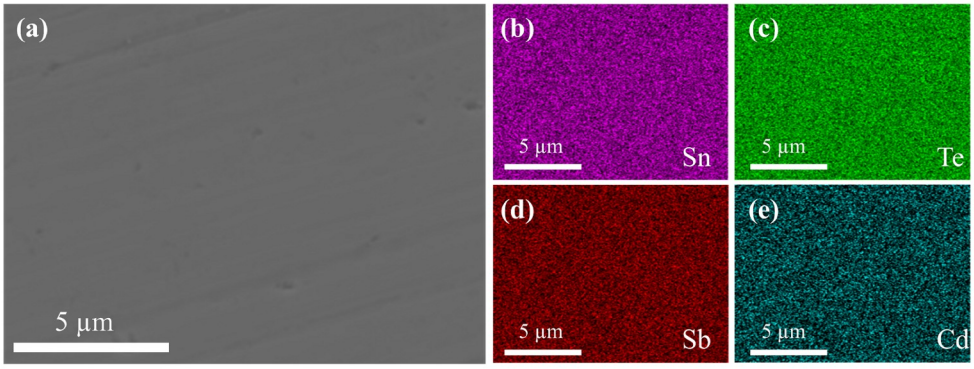


图 2 (网络版彩色)$Sb_2Te_3(Sn_{0.96}Cd_{0.04}Te)_6$样品抛光表面的SEM图(a), 以及对应的Sn、Te、Sb和Cd元素分布图谱(b~e)
Figure 2 (Color online) The SEM image of the polished surface for $Sb_2Te_3(Sn_{0.96}Cd_{0.04}Te)_6$ sample (a), and the corresponding elemental distributions for Sn, Te, Sb, and Cd (b–e)

运性能随温度的变化曲线. 从图3(a)可以看出, 所有样品的电导率均随温度的升高而降低, 展现出典型的简并半导体输运行为. 此外, 随着Cd掺杂含量的增加, 样品的电导率也逐渐降低. 室温电导率从$Sb_2Te_3(SnTe)_6$样品的1349 S cm^{-1}降低到$Sb_2Te_3(Sn_{0.92}Cd_{0.08}Te)_6$样品的867 S cm^{-1}. 为了探究电导率变化的具体原因, 我们测试了$Sb_2Te_3(Sn_{1-x}Cd_xTe)_6$ (x=0~0.08)样品的室温霍尔载流子浓度和载流子迁移率, 如图3(b)所示. 随着Cd掺杂含量的增加, 载流子迁移率略有下降并维持在相对稳定的水平; 而载流子浓度连续下降, 室温载流子浓度由$Sb_2Te_3(SnTe)_6$的8.95 × 10^{20} cm^{-3}降低到$Sb_2Te_3(Sn_{0.92}Cd_{0.08}Te)_6$的6.54 × 10^{20} cm^{-3}. 由此看来, 电导率降低主要是载流子浓度的降低导致的. 载流子浓度的降低可能是由于Cd元素的掺杂提高了Sn空位的形成能[30]. 可以看到, 所有$Sb_2Te_3(Sn_{1-x}Cd_xTe)_6$ (x=0~0.08)样品的电导率远低于未掺杂的SnTe材料, 这主要是由于大量的阳离子空位增强了对载流子的散射, 导致$Sb_2Te_3(Sn_{1-x}Cd_xTe)_6$样品的载流子迁移率远低于SnTe.

图3(c)是$Sb_2Te_3(Sn_{1-x}Cd_xTe)_6$ (x=0~0.08)样品的塞贝克系数随温度变化曲线, 所有样品的塞贝克系数均为正值, 表明材料为p型半导体. 另外, $Sb_2Te_3(SnTe)_6$样品的塞贝克系数远高于未掺杂的SnTe样品, 这主要是由于合金化Sb_2Te_3后促进了轻重价带的收敛, 提高了能带简并度[27]. 随着Cd掺杂含量的增加, 塞贝克系数逐渐升高, 室温塞贝克系数由$Sb_2Te_3(SnTe)_6$样品的80 μV K^{-1}提高至$Sb_2Te_3(Sn_{0.92}Cd_{0.08}Te)_6$样品的103 μV K^{-1}. 载流子浓度和塞贝克系数可以通过以下公式[7,31]进行关联:

$$S = \pm\frac{k_B}{e}\left(\frac{(r+5/2)F_{r+2/3}(\eta)}{(r+3/2)F_{r+1/2}(\eta)} - \eta\right), \quad (1)$$

$$n = 4\pi\left(\frac{2m^*k_BT}{h^2}\right)^{3/2}F_{1/2}(\eta), \quad (2)$$

$$F_n(\eta) = \int_0^\infty \frac{x^n}{1+e^{x-\eta}}dx, \quad (3)$$

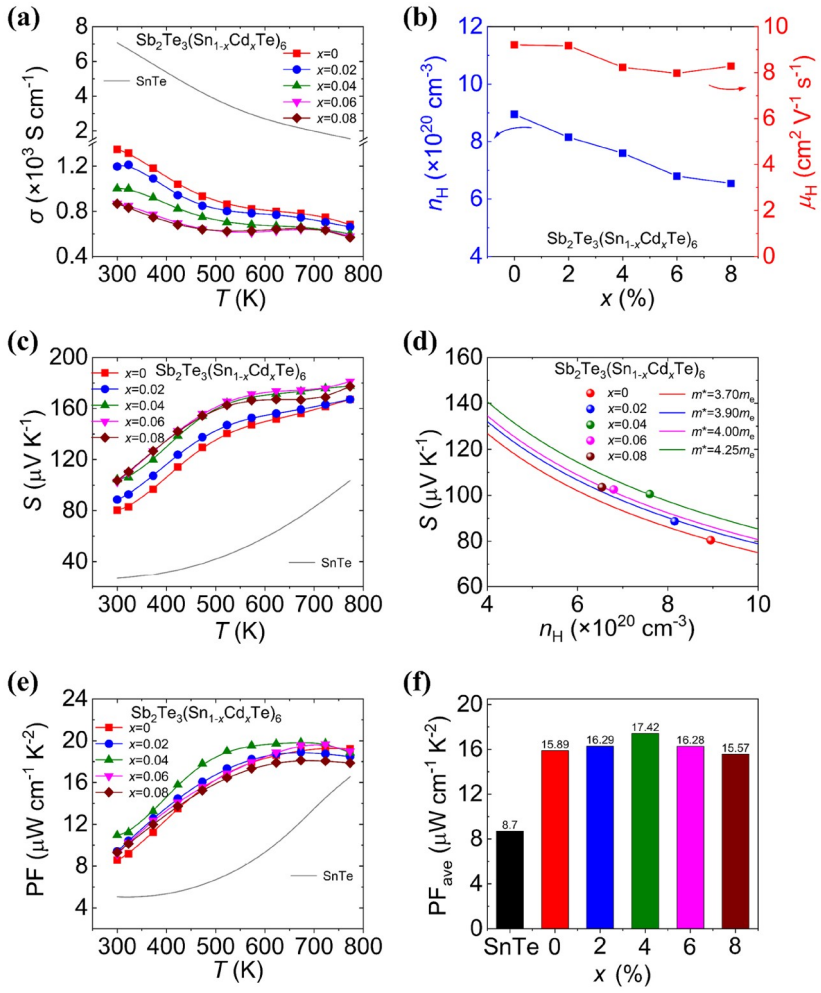


图 3 (网络版彩色)$Sb_2Te_3(Sn_{1-x}Cd_xTe)_6$ (x=0~0.08)样品的电输运性能. (a) 电导率; (b) 室温霍尔载流子浓度与迁移率; (c) Seebeck系数; (d) 基于单抛物带模型计算的Pisarenko曲线, 以及样品的室温塞贝克系数随载流子浓度的变化; (e) 功率因子; (f) 300~773 K温度范围的平均功率因子

Figure 3 (Color online) The electrical transport properties of $Sb_2Te_3(Sn_{1-x}Cd_xTe)_6$ (x=0–0.08) samples. (a) Electrical conductivity; (b) room-temperature Hall carrier concentration and carrier mobility; (c) Seebeck coefficients; (d) the Pisarenko curve based on single parabolic band model and the variation of Seebeck coefficients with carrier concentration at room temperature; (e) power factor; (f) average power factor from 300 to 773 K temperature range

式中, η是简约费米能级, k_B是玻尔兹曼常数, r是散射因子, h是普朗克常数, $F_n(\eta)$是费米积分. 通过式(1)~(3)计算了$Sb_2Te_3(Sn_{1-x}Cd_xTe)_6$ (x=0~0.08)基于单抛物带(single parabolic band)模型对应的理论Pisarenko曲线[32,33], 如图3(d)所示, 其中实线为计算得到的塞贝克系数, 对应的态密度有效质量分别为3.70 m_e、3.90 m_e、4.00 m_e和4.25 m_e. 由此可见, 随着Cd掺杂含量的增加, 样品的态密度有效质量呈现先升高后降低的趋势. 通过对载流子浓度和态密度有效质量的协同优化, $Sb_2Te_3(Sn_{1-x}Cd_xTe)_6$ (x=0~0.08)样品的功率因子得到了显著提升, 如图2(e)所示, $Sb_2Te_3(Sn_{0.96}Cd_{0.04}Te)_6$样品在300~773 K的平均功率因子高达17.42 μW cm^{-1} K^{-2}.

2.3 热输运性能

材料的总热导率通常由电子热导率(κ_{ele})和晶格热导率(κ_{lat})组成. 电子热导率由公式$\kappa_{ele}=L\sigma T$计算, 其中L代表洛伦兹常数, 由以下公式进行计算:

$$L=\left(\frac{k_B}{e}\right)^2\left\{\frac{(r+7/2)F_{r+5/2}(\eta)}{(r+3/2)F_{r+1/2}(\eta)}-\left[\frac{(r+5/2)F_{r+3/2}(\eta)}{(r+3/2)F_{r+1/2}(\eta)}\right]^2\right\}. \quad (4)$$

图4是$Sb_2Te_3(Sn_{1-x}Cd_xTe)_6$ (x=0~0.08)样品的热输运性能随温度的变化曲线. 随着Cd掺杂含量的增加, 样品的总热导率逐渐降低, 如图4(a)所示. 室温下总热导率由$Sb_2Te_3(SnTe)_6$样品的1.48 W m^{-1} K^{-1}降低到

$Sb_2Te_3(Sn_{0.92}Cd_{0.08}Te)_6$样品的1.09 W m^{-1} K^{-1}. 总热导率由晶格热导率(κ_{lat})和电子热导率(κ_{ele})组成, 通过观察图3(b)和(c)可知, 晶格热导率变化不大, 电子热导率随Cd含量的增加而逐渐下降, 因此总热导的降低主要是电子热导率降低导致的. 电子热导率的降低可以归因于Cd掺杂后载流子浓度的降低. 另外, $Sb_2Te_3(SnTe)_6$样品的晶格热导率远低于未掺杂的SnTe, 如图4(c)所示, 室温晶格热导率由SnTe的3.12 W m^{-1} K^{-1}大幅下降至$Sb_2Te_3(SnTe)_6$样品的0.66 W m^{-1} K^{-1}, 这是因为合金化后引入了大量的Sn空位和范德华面间隙结构等, 从而有效地散射了不同频率的声子, 极大降低了材料的晶格热导率[27].

图4(d)绘制了$Sb_2Te_3(Sn_{1-x}Cd_xTe)_6$ (x=0~0.08)样品的ZT值随温度的变化曲线. 由于Cd掺杂实现了功率因子和总热导率的协同优化, 获得了较高的室温ZT和平均ZT值. $Sb_2Te_3(Sn_{0.96}Cd_{0.04}Te)_6$样品的室温$ZT$值达到了0.26, 323~773 K温度范围的平均ZT值达到了0.79. 图5绘制了本工作同其他合金化后SnTe基材料热电性能的

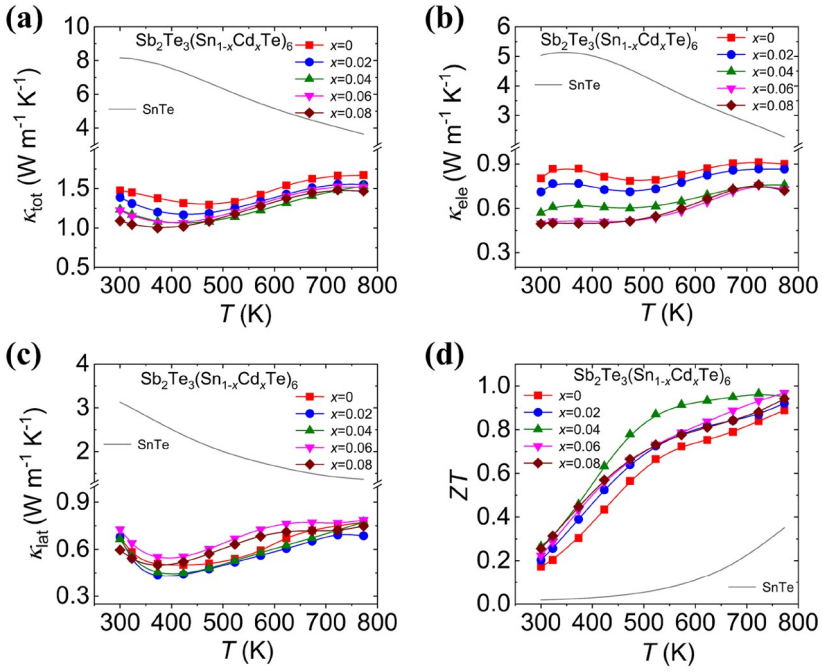


图 4 (网络版彩色)$Sb_2Te_3(Sn_{1-x}Cd_xTe)_6$ (x=0~0.08)样品的热电输运性能. (a) 总热导率; (b) 电子热导率; (c) 晶格热导率; (d) 热电优值

Figure 4 (Color online) The thermoelectric transport properties of $Sb_2Te_3(Sn_{1-x}Cd_xTe)_6$ (x=0–0.08) samples. (a) Total thermal conductivity; (b) electronic thermal conductivity; (c) lattice thermal conductivity; (d) ZT values

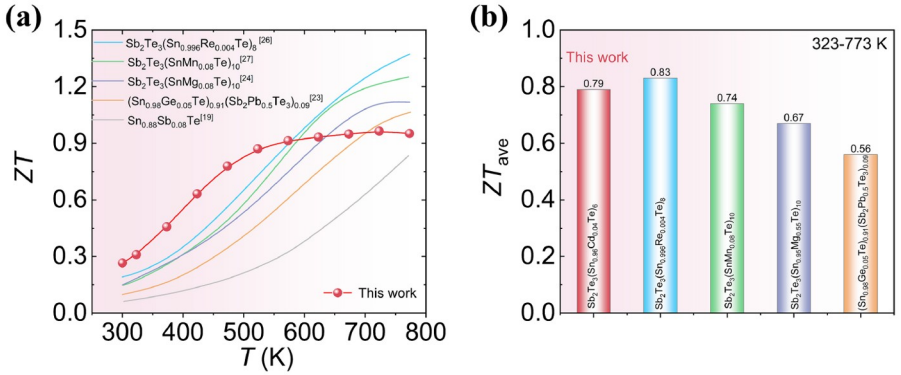


图 5 (网络版彩色)本工作ZT与其他合金化Sb_2Te_3工作对比图(a), 以及平均ZT对比图(b)

Figure 5 (Color online) Comparison of temperature-dependent ZT values (a) and average ZT values (b) from our work and previously reported data for the alloying Sb_2Te_3 system

对比. 可以看出, 本工作主要提高了SnTe在近室温区(300~500 K)的热电性能, 这将有利于材料在低品位废热利用和热电制冷领域的应用.

3 结论

本文通过高温熔融和放电等离子体烧结技术制备了一系列$Sb_2Te_3(Sn_{1-x}Cd_xTe)_6$ (x=0~0.08)样品. 通过在合金化Sb_2Te_3基础上掺杂Cd元素, 协同优化了Sb_2Te_3-$(SnTe)_6$的载流子浓度、态密度有效质量以及晶格热导率, 显著提高了其热电性能. 最终$Sb_2Te_3(Sn_{0.96}Cd_{0.04}Te)_6$样品的室温$ZT$值达到了0.26, 323~773 K温度范围内的平均ZT值达到了0.79. 考虑到$Sb_2Te_3(SnTe)_6$材料的窄带隙特性, 高温下易发生双极扩散现象, 限制了其高温热电性能的提升. 因此, 未来可以通过合金化增大带隙的方法抑制双极扩散效应, 有望进一步提升其宽温域热电性能.

参考文献

1 Xiao Y, Zhao L D. Seeking new, highly effective thermoelectrics. Science, 2020, 367: 1196–1197
2 Su L, Wang D, Wang S, et al. High thermoelectric performance realized through manipulating layered phonon-electron decoupling. Science, 2022, 375: 1385–1389
3 Qin B, Zhao L D. Moving fast makes for better cooling. Science, 2022, 378: 832–833
4 Qin Y, Qin B, Wang D, et al. Solid-state cooling: Thermoelectrics. Energy Environ Sci, 2022, 15: 4527–4541
5 Liu Z, Hong T, Xu L, et al. Lattice expansion enables interstitial doping to achieve a high average *ZT* in n-type PbS. Interdisciplinary Mater, 2022, 2: 161–170
6 Wang C L. Recent progress in thermoelectric materials, devices and applications (in Chinese). Chin Sci Bull, 2021, 66: 2024–2032 [王春雷. 热电材料、器件设计和应用新进展. 科学通报, 2021, 66, 2024–2032]
7 Qian X, Wu H, Wang D, et al. Synergistically optimizing interdependent thermoelectric parameters of n-type PbSe through alloying CdSe. Energy Environ Sci, 2019, 12: 1969–1978
8 Qian X, Wang D, Zhang Y, et al. Contrasting roles of small metallic elements M (M = Cu, Zn, Ni) in enhancing the thermoelectric performance of n-type $PbM_{0.01}Se$. J Mater Chem A, 2020, 8: 5699–5708
9 Gao D, Wang S, Wen Y, et al. Enhancing thermoelectric properties of ductile $Ag_2S_{0.7}Te_{0.3}$ with trace Ag vacancy. Mater Today Phys, 2024, 41: 101353
10 Moshwan R, Yang L, Zou J, et al. Eco-friendly SnTe thermoelectric materials: Progress and future challenges. Adv Funct Mater, 2017, 27: 1703278
11 Li W, Wu Y, Lin S, et al. Advances in environment-friendly SnTe thermoelectrics. ACS Energy Lett, 2017, 2: 2349–2355
12 Hong T, Wang D, Qin B, et al. Band convergence and nanostructure modulations lead to high thermoelectric performance in $SnPb_{0.04}Te$-y% $AgSbTe_2$. Mater Today Phys, 2021, 21: 100505
13 Zhao L D, Wu H J, Hao S Q, et al. All-scale hierarchical thermoelectrics: MgTe in PbTe facilitates valence band convergence and suppresses bipolar thermal transport for high performance. Energy Environ Sci, 2013, 6: 3346–3355
14 Zhao L D, Dravid V P, Kanatzidis M G. The panoscopic approach to high performance thermoelectrics. Energy Environ Sci, 2014, 7: 251–268
15 Guo C R, Qin B C, Wang D Y, et al. Investigation on halogen-doped n-type SnTe thermoelectrics. Rare Met, 2022, 41: 3803–3814
16 Hong T, Guo C, Wang D, et al. Enhanced thermoelectric performance in SnTe due to the energy filtering effect introduced by Bi_2O_3. Mater Today Energy, 2022, 25: 100985
17 Hong T, Guo C, Qin B, et al. Realizing ultrahigh room-temperature seebeck coefficient and thermoelectric properties in SnTe-based alloys through carrier modulation and band convergence. Acta Mater, 2023, 261: 119412
18 Qian X, Guo H R, Lyu J X, et al. Enhancing thermoelectric performance of p-type SnTe through manipulating energy band structures and decreasing electronic thermal conductivity. Rare Met, 2024, 43: 3232–3241
19 Lyu T, Yang Q, Meng F, et al. Enhancing thermoelectric performance of $Sn_{1-x}Sb_{2x/3}Te$ via synergistic charge balanced compensation doping. Chem Eng J, 2021, 404: 126925
20 Tan G, Shi F, Hao S, et al. Codoping in SnTe: Enhancement of thermoelectric performance through synergy of resonance levels and band convergence. J Am Chem Soc, 2015, 137: 5100–5112
21 Pei Y, Shi X, LaLonde A, et al. Convergence of electronic bands for high performance bulk thermoelectrics. Nature, 2011, 473: 66–69
22 Zhang Q, Guo Z, Wang R, et al. High-performance thermoelectric material and module driven by medium-entropy engineering in SnTe. Adv Funct Mater, 2022, 32: 2205458
23 Min Y, Kim M, Hwang G T, et al. Vacancy engineering in rock-salt type $(IV\text{-}VI)_x(V\text{-}VI)$ materials for high thermoelectric performance. Nano Energy, 2020, 78: 105198

24 Yang Z, Smith E, Tseng Y C, et al. Band and vacancy engineering in SnTe to improve its thermoelectric performance. J Mater Chem A, 2024, 12: 5357–5365

25 Wang J, Yu Y, He J, et al. Synergy of valence band modulation and grain boundary engineering leading to improved thermoelectric performance in SnTe. ACS Appl Energy Mater, 2021, 4: 14608–14617

26 Xu X, Cui J, Huang Y, et al. Microstructural manipulation for enhanced average thermoelectric performance: A case study of tin telluride. ACS Appl Mater Interfaces, 2023, 15: 9656–9664

27 Xu X, Cui J, Yu Y, et al. Constructing van der Waals gaps in cubic-structured SnTe-based thermoelectric materials. Energy Environ Sci, 2020, 13: 5135–5142

28 Xia J, Huang Y, Xu X, et al. Fine electron and phonon transports manipulation by Mn compensation for high thermoelectric performance of $Sb_2Te_3(SnTe)_n$ materials. Mater Today Phys, 2023, 33: 101055

29 Qin B, Wang D, Liu X, et al. Power generation and thermoelectric cooling enabled by momentum and energy multiband alignments. Science, 2021, 373: 556–561

30 Tan G, Zhao L D, Shi F, et al. High thermoelectric performance of p-type SnTe via a synergistic band engineering and nanostructuring approach. J Am Chem Soc, 2014, 136: 7006–7017

31 Qian X, Zhang X, Guo H, et al. Enhancing thermoelectric performance of n-type $AgBi_3S_5$ through synergistically optimizing the effective mass and carrier mobility. J Materiomics, 2023, 9: 874–881

32 Zhao L D, He J, Hao S, et al. Raising the thermoelectric performance of p-type PbS with endotaxial nanostructuring and valence-band offset engineering using CdS and ZnS. J Am Chem Soc, 2012, 134: 16327–16336

33 Lee K H, Kim S, Lim J, et al. Approach to determine the density-of-states effective mass with carrier concentration-dependent seebeck coefficient. Adv Funct Mater, 2022, 32: 2203852

Summary for “掺杂Cd元素协同优化$Sb_2Te_3(SnTe)_6$的热电输运性能”

Synergistic optimization of thermoelectric transport properties in $Sb_2Te_3(SnTe)_6$ through Cd doping

Yuqing Liu, Jinhua Cui, Shu-Fang Wang* & Xin Qian*

Hebei Key Lab of Optic-Electronic Information and Materials, College of Physics Science and Technology, Hebei University, Baoding 071002, China
* Corresponding authors, E-mail: sfwang@hbu.edu.cn; qianxin@hbu.edu.cn

Under the background of a worsening energy crisis, there is an increasing global demand for efficient and environmentally friendly energy conversion methods. Thermoelectric materials, which are capable of bidirectional conversion between thermal energy and electrical energy, show significant potential for applications in waste heat utilization and solid-state refrigeration technology. Thermoelectric materials offer innovative solutions to the current energy shortage. SnTe and PbTe share the same crystal structure and similar two-valence-band structure, but SnTe does not contain the toxic element Pb, has attracted great attention and research interest. Despite exhibiting relatively high thermoelectric performance in the medium to high-temperature range, enhancing the thermoelectric performance of SnTe near room temperature poses a challenge primarily due to its excessively high carrier concentration and low Seebeck coefficient. As the advancement of thermoelectric cooling technology continues, the performance of materials at room temperature becomes increasingly crucial. Previous studies have demonstrated that alloying with Sb_2Te_3 introduces a significant number of cation vacancies and dislocation defects, effectively reducing the lattice thermal conductivity of SnTe. This process also enables the modulation of the band structure, thereby increasing the effective mass, which has been demonstrated as a successful strategy for enhancing thermoelectric performance across a broad temperature range. Relevant research indicates that $Sb_2Te_3(SnTe)_6$ exhibits superior room temperature thermoelectric performance and average thermoelectric performance compared to other alloyed samples. Therefore based on the Sb_2Te_3 alloying approach, this study incorporates Cd doping at the Sn site to synergistically regulate the carrier concentration, density of states effective mass, and lattice thermal conductivity of $Sb_2Te_3(SnTe)_6$.

Thermoelectric materials, $Sb_2Te_3(Sn_{1-x}Cd_xTe)_6$ (x=0–0.08) were synthesized by vacuum melting and spark plasma sintering (SPS). The vacuum melting reactions were heated from room temperature to 1423 K over 16 hours, maintained at this temperature for 24 hours, then slowly cooled to 873 K over 6 hours, and finally cooled down to room temperature. The compounds were fully characterized by a range of techniques, including X-ray diffraction, energy dispersive spectrometer, and Hall coefficient test system, etc. The X-ray diffraction and energy dispersive spectrometer results demonstrate that Cd was successfully incorporated into $Sb_2Te_3(SnTe)_6$. The Hall coefficient test indicates that the substitution of Cd results in an obvious decrease in the carrier concentration. The Pisarenko curves calculated based on the single parabolic band model demonstrate that the effective mass increases with an increase in Cd content. The experimental results show that the effective mass of $Sb_2Te_3(SnTe)_6$ and the carrier concentration are co-optimized by doping Cd at the Sn position, and the thermoelectric transport performance of the material is significantly improved over the whole temperature range.

In conclusion, this study incorporates Cd doping at the Sn site to synergistically regulate the carrier concentration, density of states effective mass, and lattice thermal conductivity of $Sb_2Te_3(SnTe)_6$. As a result, the ZT value of Sb_2Te_3-$(Sn_{0.96}Cd_{0.04}Te)_6$ reached 0.26 at 300 K, with an average ZT value of 0.79 in the temperature range of 323–773 K. The results indicate that SnTe-Sb_2Te_3 compounds exhibit significant potential for utilization in thermoelectric power generation and cooling applications.

thermoelectric materials, carrier concentration, effective mass, lattice thermal conductivity, thermoelectric performance

doi: 10.1360/TB-2024-0776